

Contents lists available at [SciVerse ScienceDirect](http://www.sciencedirect.com)

## Chemical Engineering Research and Design

journal homepage: [www.elsevier.com/locate/cherd](http://www.elsevier.com/locate/cherd)

IChemE

# Simulation study and kinetic parameter estimation of underground coal gasification in Alberta reservoirs

Mohammad Kariznovi, Hossein Nourozieh, Jalal Abedi\*, Zhangxin Chen

Department of Chemical & Petroleum Engineering, University of Calgary, Calgary, Canada

## ABSTRACT

A new method is developed for the estimation of chemical reaction kinetics at high-pressure underground coal gasification from the field produced gas composition. This method combines a developed numerical forward model and field data to investigate uncertain parameters. The forward model is developed on the basis of a unique porous media approach that combines the effects of heat, mass transport, and chemical reactions to simulate the underground coal gasification in three-dimensional basis. The chemical reaction kinetics, that is limited to low pressure, is upscaled based on the available experimental data. A comprehensive sensitivity analysis is carried out to estimate the reaction kinetics and investigate the effect of various parameters, such as pressure, temperature, and reaction environment, on the produced gas composition. The novelty of the developed method is in its applicability as well as its ability to generate the chemical reaction kinetics that corresponds to the field under study. The advantage of the proposed technique is that the sensitivity of the model to different kinetic parameters can be investigated by a graphical method.

© 2012 The Institution of Chemical Engineers. Published by Elsevier B.V. All rights reserved.

**Keywords:** Underground coal gasification; Parameter estimation; Reaction kinetics; Forward model; Porous media approach; Three-dimensional model

## 1. Introduction

Coal is a major fossil fuel and plays a demanding role in the energy sector. Canada is ranked tenth worldwide in coal reserves, and Alberta's 33.6 billion tons of proven mineable coal represents 70% of Canada's reserves. The deep, stranded coal reserves in Canada, which are not part of the coal reserve base, exceed 600 billion tons in Alberta alone ([Energy Resources Conservation Board, 2008](#)). Consequently, Alberta's coal resources constitute an enormous source of untapped energy; thus there is a need for the development of novel technologies for the efficient and clean utilization of coal.

Underground coal gasification (UCG) can be considered as a technique that can be applied to convert the abundant coal resources into a synthetic gas. The process involves the injection of steam and air or oxygen into an underground coal seam to ignite and burn coal in situ to produce a combustible gas that can be used either as a fuel or chemical feedstock. UCG has the advantages of high safety, high efficiency, low cost, environmentally friendliness, and a high return rate,

compared with surface gasification ([Gregg and Edgar, 1978; Burton et al., 2006; Shafirovich and Varma, 2009](#)). In addition, it can be applied to deep and thin coal seams that are not economical for mining.

Accurate production prediction and process optimization are essential to correctly interpret pilot and field data, leading to a better understanding and design of the process in the field. Mathematical models and numerical simulations, as a preliminary study, give better insights to the process. While there have been extensive models for the gasification of coal in one dimension, there are relatively few on the modeling of the process in the three-dimensional space or the field scale. A distinguishing feature of three-dimensional modeling is that the physical and chemical phenomena, such as mass and heat transport, chemical reactions, and geomechanical behavior, become far more complex.

Despite the complexity of the process in the field scale, there are no numerical investigations into the gasification of coal at very high pressure (>10 MPa) and depth (>1000 m). Numerical models developed by [Massaquoi and](#)

\* Corresponding author at: 2500 University Dr., NW, Calgary, Alberta T2N 1N4, Canada. Tel.: +1 403 220 5594.

E-mail address: [jabedi@ucalgary.ca](mailto:jabedi@ucalgary.ca) (J. Abedi).

Received 14 February 2012; Received in revised form 25 October 2012; Accepted 13 November 2012

0263-8762/\$ – see front matter © 2012 The Institution of Chemical Engineers. Published by Elsevier B.V. All rights reserved.

<http://dx.doi.org/10.1016/j.cherd.2012.11.008>

**Nomenclature**

A	flow area
B	reaction components
C	solid concentration
D	diffusion coefficient
E	activation energy
H	enthalpy
J	sensitivity matrix
k	permeability
$k_r$	relative permeability
l	distance
M	objective function
N	number of moles
n	number of components
q	injection or production rate
R	gas constant
r	rate of creation and destruction
S	fluid saturation
s	stoichiometric coefficient
T	temperature
t	time
U	internal energy
V	block volume
y	mole fraction
CMG	computer modeling group
exp	experiment
GC	gas composition
LMA	Levenberg–Marquardt algorithm
SAGD	steam assisted gravity drainage
UCG	underground coal gasification

**Greek letters**

$\chi$	stopping criteria
$\varepsilon$	reaction rate
$\phi$	porosity
$\varphi$	flow potential
$\eta$	reaction order
$\kappa$	thermal conductivity
$\lambda$	transmissibility
$\mu$	fluid viscosity
$\rho$	density
$\sigma$	adjusting parameter
$\omega$	matrix of gas composition
$\xi$	volatile content of coal
$\Omega$	diagonal matrix

**Subscripts**

f	fluid
g	gas
s	solid
v	iteration number
W	water

One of the major processes in UCG is chemical reaction. The dependence of chemical reactions on the coal block size and the environmental condition in which the chemical reaction occurs can affect the process. The former was studied by Nourozieh et al. (2010) and it was shown that the temperature distribution and chemical process behavior depend on the coal block size. For the latter, experimental study is essential for the modeling of reactions. Most experiments on char reactions have been done at atmospheric conditions and there are only a limited number of studies that measure the kinetics rate of char reaction at high pressure (MacNeil and Basu, 1998; Monson et al., 1995; Roberts and Harris, 2000; Muhlen et al., 1985).

The above-mentioned studies encouraged us to find a parameter estimation method for investigating the chemical reaction kinetics based on field history data. In this method, reaction parameters, which were obtained at low pressures and in laboratory scale, are upscaled and estimated for the field scale. From an engineering point of view, this is an inverse problem.

Generally, two different kinds of problems are considered in engineering – forward and inverse (Schulze-Riegert et al., 2003). For a forward problem, the task is the determination of the model response from the input. In this approach, input data are introduced to the model, which generates the response as output. In an inverse problem, the aim is the determination of model parameter(s) within a certain domain from data, and information may give the boundary of this domain.

Several techniques, such as the Newton method, the steepest descent method, the Levenberg–Marquardt, random search, and genetic algorithms can be used for solving an inverse problem. Some of these methods, such as the random search and genetic algorithms, require many sets of estimated parameters. These methods are not applicable for UCG, where the computational time is too high. Thus it is essential to select a method that has a high convergence rate to estimate parameters with a minimum number of runs. To satisfy the above criteria, the Levenberg–Marquardt method (Levenberg, 1944; Marquardt, 1963) is preferred for parameter estimation.

The objective of the present work is the combination of the developed forward model with field data to investigate uncertain parameters. To this aim, first a three-dimensional model for underground coal gasification in Alberta reservoir is developed. Then, the sensitivity of the model to different kinetic parameters is investigated by a graphical method. Finally, the chemical processes' kinetics based on the literature experimental data are evaluated and estimated for the field under study.

## 2. UCG forward model

In this study, computer modelling group (CMG)'s software STARS is used to build up forward model and study of UCG in deep coal seams. STARS is a semi-compositional porous media based simulator that combines the heat and mass transport equations with chemical reactions to investigate the UCG process. This software as a commercial tool, was developed to simulate the processes such as steam flood, steam cycling, SAGD (steam assisted gravity drainage), dry and wet combustion, along with many types of chemical processes, using a wide range of grid and porosity models in both field and laboratory scale (Computer Modelling Group Ltd., <http://www.cmgl.ca/software/stars.htm>).

Riggs (1983a,b), Park and Edgar (1987), Tsang (1980), and Perkins and Sahajwalla (2005) are for one-dimensional coal gasification up to a pressure of 5 MPa. In some areas, e.g., in Alberta, there are some coal seams in which the coal gasification occurs in situ at a pressure of around 12 MPa, which is substantially higher than the previously cited numerical studies.




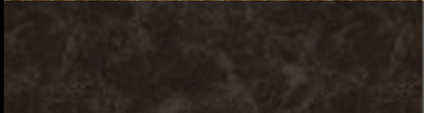



SEAM SUBVISION			
Coal Layering	Thickness [m]	Seam Name	Comment
	0.5	Roof	Claystone
	3.5	Upper Subseam	20 cm of upper subseam assigned to the middle seam
	0.5	Interspersed layer	Claystone
	1.5	Middle Subseam	
	0.5	Interspersed layer	Claystone
	2	Lower Subseam	The thickness of thin subseam added to the lower seam
	0.5	Floor	Claystone

Fig. 1 – Coal seam layers considered in three-dimensional model (Nourozieh et al., 2010).

The developed forward model was described in detail elsewhere (Nourozieh et al., 2010) which includes the geological structure, permeability/porosity variation, chemical reactions, transport equations, and ignition procedure. The main focus in this study is on the three-dimensional UCG forward model and the developed kinetic parameter estimation method; therefore, the geological structure, ignition procedure, chemical processes, and governing equations described in the previous study (Nourozieh et al., 2010) are applied and a three-dimensional UCG model based on the governing equations explained in Section 2 is used for simulation study.

### 2.1. Geological structure

The coal seam under study is 9 m thick; Fig. 1 shows the coal and claystone layers. The layers interspersed between coal seams are mostly claystone with 0.5 m thickness. The overall thickness of coal layers is 7 m, and the upper subseam coal layer is the thickest (3.5 m). The average proximate analysis of the coal under study is summarized in Table 1. The coal is a highly volatile bituminous with a fixed high carbon content and the interspersed layers are mostly claystone.

### 2.2. Three-dimensional model

The coal seam under study is deep and consists of thin layers; thus, the CRIPS technique is appropriate and considered

in the model. Fig. 2 shows the physical model as well as the wells configuration. The distance between the injector toe and the producer is 4 m and the coal seam consists of three layers which are identified in red color in Fig. 2. The producer is just perforated in the bottom coal layer. Table 2 summarizes the seam and model properties. This model assumes that there is no heat loss or water influx from the adjacent area. The permeability of the coal layers is about 1 millidarcy (mD) and the initial communication between the injector and producer is created by a fracture so a layer of high permeability that connects the injector to the producer is developed in the model.

### 2.3. Chemical processes

Three different zones in UCG process occur: drying, pyrolysis, and combustion and gasification of solid char. In the first zone (drying or evaporation), wet coal is converted into dry coal

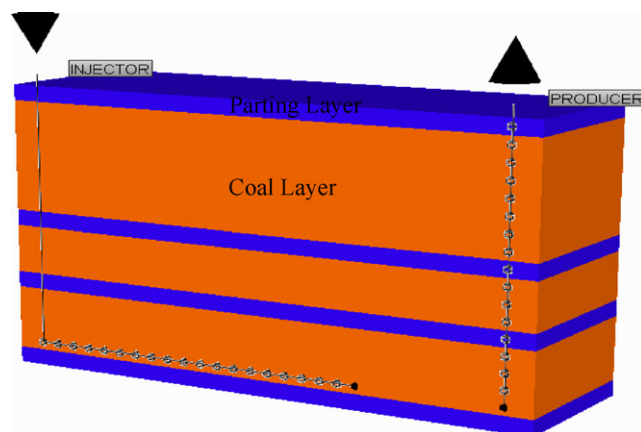


Fig. 2 – Three-dimensional model and corresponding layers (Nourozieh et al., 2010).

Table 1 – Average proximate analysis for coal and claystone layers (Nourozieh et al., 2010).

	Coal	Claystone
Fixed carbon	55.61	4.92
Volatile matter	30.36	9.05
Ash	9.20	82.88
Moisture	4.83	3.15

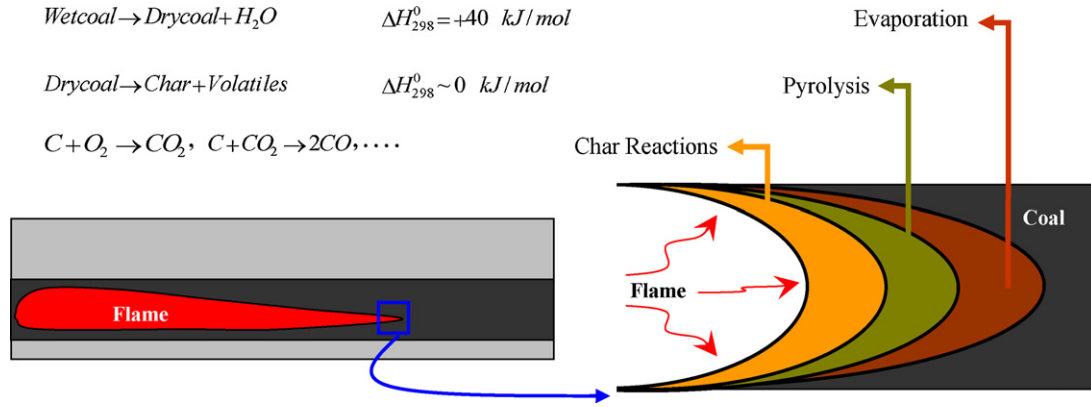


Fig. 3 – Different regions during underground coal gasification (Nourozieh et al., 2010).

by increasing the temperature over  $100^\circ\text{C}$  (Lyczkowski, 1978). During pyrolysis, coal loses its weight, generating volatile matters and solid that is called char. Finally, the char reacts with the injected/pyrolyzed gases to produce the syngas. Fig. 3 shows these regions during coal gasification in situ.

### 2.3.1. Pyrolysis

Pyrolysis is the decomposition of coal by increasing the temperature above pyrolysis temperature and results in a series of reactions releasing volatile gases from the porous coal matrix, over the temperature range  $400\text{--}900^\circ\text{C}$  (Anthony and Howard, 1976):



The yields of volatiles and their composition depend on the volatile matter content of coal, temperature, and pressure during the process. Furthermore, different gases are evolved at different temperatures during this process (Campbell, 1978). To evaluate each gas component, a kinetic model for this component is required, leading to a system of parallel reactions with different kinetic parameters (Tsang, 1980). To simplify the process, pyrolysis is modeled by a simple first-order Arrhenius expression as,

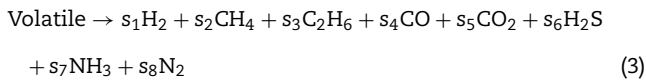
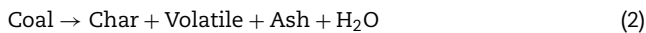


Table 2 – Model parameters for UCG (Nourozieh et al., 2010).

Parameter	Value
Initial reservoir temperature	$60^\circ\text{C}$
Initial reservoir pressure	$11.5 \text{ Mpa}$
Coal permeability	$1 \text{ mD}$
Claystone permeability	$0.1 \text{ mD}$
Coal porosity, fraction	$0.0866$
Claystone porosity, fraction	$0.05$
Thickness	$9 \text{ m}$
Number of coal layers	$3$
Initial water saturation, fraction	$0.7$
Number of grids (uniform)	$10,800$
Injected fluid	Water/oxygen

where the rate of volatile matter lost is (Van Krevelen et al., 1951),

$$\frac{d\xi}{dt} = \varepsilon(\xi^0 - \xi) \quad (4)$$

$\xi$ , volatile lost, fraction of the original coal weight;  $\xi^0$ , effective volatile content of the coal.

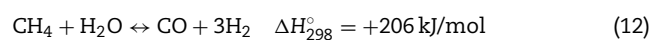
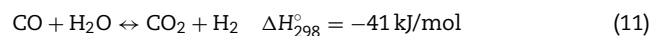
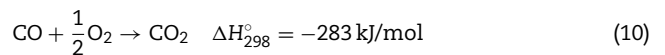
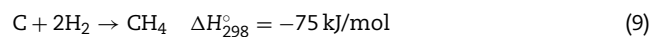
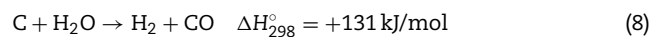
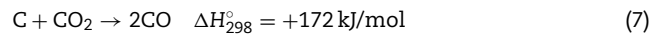
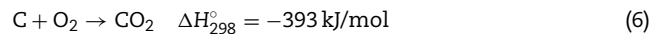
The rate constant in Eq. (4) is typically correlated with temperature by

$$\varepsilon = \varepsilon_0 \exp\left(-\frac{E}{RT}\right) \quad (5)$$

Using proximate and ultimate analysis of the coal, the stoichiometric coefficients will be obtained based on the mass balance equations for each element (Nourozieh et al., 2010).

### 2.3.2. Char reactions

Char reactions are the chemical reactions occur among the gases within the cavity and carbon. The reactivity of the char to  $O_2$ ,  $H_2O$ ,  $CO_2$ , and  $H_2$  determines the rates at which the desired products are formed. Many reactions occur during this process but the most important reactions, which are considered in the model, are summarized as follows:



Reactions (6)–(8) and (10) are the main chemical reactions considered for both shallow and deep coal gasification processes. The hydrogasification (reaction (9)) is favorable at a high hydrogen pressure. In the UCG at low pressure this reaction is not significant. In presence of water, especially with low temperature, carbon monoxide-steam and methane-steam reforming reactions play an important role.



The chemical reactions are treated as the source/sink terms for each component in the model. The general heterogeneous mass transfer reaction is defined as



The kinetic model, also known as the reaction kinetics, determines the reaction speed. Its general expression is

$$r_{k,chem} = \varepsilon_{f,k} \prod_{j=1}^n C_j^{\eta_{j,k}} \quad (14)$$

In addition, the rate of creation and destruction of the  $i$ th species in reaction  $k$  is given by

$$r_{i,k} = (s'_{i,k} - s_{i,k}) \left( \varepsilon_{f,k} \prod_{j=1}^n C_j^{\eta_{j,k}} \right) \quad (15)$$

Defining the net stoichiometric coefficient as  $s''_{i,k} = s'_{i,k} - s_{i,k}$ , the rate of creation/destruction can be written as

$$r_{i,k} = s''_{i,k} \cdot r_{k,chem} \quad (16)$$

In some cases such as solid gasification, the term  $C_j$  in Eq. (15) is replaced by the partial pressure of reacting gas. The forward reaction rate  $\varepsilon_{f,k}$  is assumed to have a simple Arrhenius form:

$$\varepsilon_{f,k} = \varepsilon_{0,k} \exp \left( -\frac{E_k}{RT} \right) \quad (17)$$

where the activation energy  $E_k$  determines the temperature dependence of  $r_{i,k}$ .

## 2.4. Governing equations

Two main transport phenomena in UCG are mass and heat transfer processes. Indeed, the UCG performance and chemical process behavior are controlled by heat and mass phenomena. In the model, these conservation equations are defined in three dimensional spaces. The convective flow for gas species inside the cavity is based on Darcy's law. For heat transport, the convection and conduction are considered as the main heat transfer processes in the UCG model.

The mass conservation equation for component  $i$  is

$$\Delta \lambda_w y_{i,w} \Delta \varphi_w + \Delta \lambda_g y_{i,g} \Delta \varphi_g + \sum_{j=w,g} \Delta \frac{A}{\Delta l} (\rho_j D_{ij}) \Delta y_{i,j} + V \Delta (s'_{ki} - s_{ki}) r_k + q_i - \frac{V}{\Delta t} (N_i^{n+1} - N_i^n) = 0 \quad (18)$$

The first and second terms account for convective flows during the process. The third term is the mass diffusion caused by concentration variation. Mass transfer by reaction is illustrated by the forth term. Production and injection are considered by  $q_i$  and finally the last term is the accumulation term.

The transmissibility  $\lambda_j$  is defined as

$$\lambda_j = \left( \frac{kA}{\Delta l} \right) \left( \frac{k_{rj} \rho_j}{\mu_j} \right) \quad (19)$$

which depends on the permeability, densities, viscosities, and grid block size.

For the solid components, only accumulation by combustion of solid is considered. As the pyrolysis or the char gasification takes place, the solid concentration inside the reservoir is changed. The dependence of the solid concentration on chemical processes is given by

$$V \frac{\partial}{\partial t} [\phi_v C_i] = V \Delta (s'_{i,k} - s_{i,k}) r_k \quad (20)$$

which shows the variation of solid with respect to time.

The energy conservation equation is

$$\Delta \lambda_w H_w \Delta \varphi_w + \Delta \lambda_g H_g \Delta \varphi_g + \Delta (\kappa \Delta T) + \sum_{j=w,g} \rho_j q_j H_j + V \Delta (H_{r,k} r_k) - V \frac{\partial}{\partial t} \left\{ \phi_f \left[ \sum_{j=w,g} \rho_j S_j U_j \right] + \phi_v C_s U_s + (1 - \phi_v) U_r \right\} = 0 \quad (21)$$

The first and second terms are the flow terms of energy; heat transport by conduction is illustrated by the third term. The well source/sink term for energy is the forth term. The reaction source/sink term for energy is the fifth term and the accumulation term for energy is the last term in the above equation. Here, the heat lose term is not considered; an isolated model is assumed. The transmissibility,  $\lambda_k$ , is defined in Eq. (19).

## 3. Challenges in simulation of UCG

### 3.1. Coal block size

The blocks of coal, which are considered in the forward model, are  $0.5 \text{ m} \times 0.5 \text{ m} \times 0.5 \text{ m}$  in size. The sensitivity study for this model resulted in variation of the temperature distribution and consequently, chemical processes. The size of the coal blocks affects the behavior of the conversion process and gasification. The experimental data obtained are based on fine particles under laboratory conditions, and these data are limited to the laboratory scale. To deal with this issue, two main approaches can be considered – resizing the grid blocks or upscaling the experimental parameters. The first approach is not appropriate for field-scale problems; reducing the grid size increases simulation time considerably and it is not practical for modeling studies. In the second approach, the experimental parameters (such as reaction kinetics) must be upscaled to be used in the simulation for field-scale modeling. This approach ensures that there is proper combustion in each field-scale grid block. Field produced gas composition is required to estimate and upscale uncertain parameters from laboratory experimental data.

### 3.2. Effect of pressure on chemical reactions

The coal seam under study has an initial pressure of about 12 MPa and the literature data on chemical reactions are limited to much lower pressures. MacNeil and Basu (1998) studied the kinetic rates of the char combustion measured at 1, 3, 5 and 7 atm. Monson et al. (1995) studied the effect of pressure (up to 15 atm) for the oxidation of very fine bituminous char at elevated pressure. These studies have resulted in almost the same conclusion that the surface reaction rates increase with pressure up to a certain pressure and then

**Table 3 – Kinetic parameters for chemical reactions occurs during UCG.**

Reaction	Reference	A	E	P, kPa	T, K
$C + O_2 \rightarrow CO_2$	Smith (1978)	3050	179.4	3–101	573–2300
	Zolin et al. (2001)	$20.9\text{--}5.31 \times 10^4$	99–208	101	973–1673
	Yang and Liu (2003)	1137	165.8	–	–
$C + CO_2 \rightarrow 2CO$	Rodriguez-Mirasol et al. (1993)	–	202–245	101	1023–1223
	Kumar and Gupta (1994)	–	138–218	101	1083–1233
	Tancredi et al. (1996)	–	230–261	101	1043–1123
	Marquez-Montesinos et al. (2002)	$4.5 \times 10^6$ to $7.37 \times 10^8$	197–249	101	998–1073
	Yang and Liu (2003)	$4.985 \times 10^{-3}$	140	–	–
$CO + 0.5O_2 \rightarrow CO_2$	Yang and Liu (2003)	$7.5 \times 10^{-2}$	247	–	–
$C + H_2O \rightarrow CO + H_2$	Hawley et al. (1983)	548	156	45–100	1073–1273
	Moilanen and Saviharju (1997)	–	217	101	973–1173
$CO + H_2O \leftrightarrow CO_2 + H_2$	Blasi (2000)	2.780	12.6	1960	1073–1223
$C + 2H_2 \rightarrow CH_4$	Shufen and Ruizheng (1994)	1717	196.6	1960	1073–1223
	Tomita et al. (1977)	$2.848 \times 10^{-2}$	150	700–2800	1148–1253
$CH_4 + H_2O \leftrightarrow CO + 3H_2$	Govind and Shah (1984)	312	30	–	–

decrease or become constant. In addition, almost all of these research works studied the reaction kinetic for each reaction individually; no one has considered the effect of other reactions on the behavior of the reaction under study.

Roberts and Harris (2000) measured the intrinsic reaction rates of two Australian coal chars (made under laboratory conditions) with oxygen, carbon dioxide, and water at increased pressures (up to 30 atm). They concluded that, for all reactions, the frequency factor does change with pressure, while the activation energy is not significantly affected by pressure. Overall, the pressure increased the rate of the char reactions for both chars, but as the pressure increased further, the effect of pressure was less. Muhlen et al. (1985) have also reported some effects of pressure on char gasification rates. They reported the reaction rates of a German char with carbon dioxide and hydrogen increasing up to 15–20 atm, and a further pressure increase (to 60 atm) had little effect, which is similar to the results reported by Roberts and Harris (2000).

The above studies concluded that reaction rates increase with increasing pressure, but the rate of increase is reduced at higher pressures or may become constant. However, there is no experimental data available under relatively high pressure (>5 MPa). Table 3 gives the kinetics parameters for different chemical reactions, which have been reported in the literature by different authors. The corresponding temperature and pressure ranges for the available data are also summarized in this table. These data are based on an Arrhenius type chemical reaction. The summarized results in Table 3 confirm that there are no available data for kinetics of chemical reactions at high pressure (>11 MPa). Thus the estimation and extrapolation of experimental parameters to high pressures (coal seam pressure) are crucial for modeling of the UCG process in deep coal seams. In this manuscript, chemical reactions are modeled by a simple Arrhenius type chemical reaction; therefore, reaction parameters, which are summarized in Table 3, can be considered as a base for upscaling and estimation of reaction kinetics for the field scale.

### 3.3. Effect of pressure on pyrolysis

The pyrolysis is modeled by a simple first-order reaction in the model (Eq. (2)). There are limited data for the behavior that coal undertakes in the pyrolysis process at high pressures. The effect of pressure on the pyrolysis was studied by Anthony et al. (1976), and they concluded that the pressure decreases the extent of pyrolysis. Makino and Toda (1979) studied the

effect of pressure on the gas evolution in pyrolysis, and they found that the pressure does not have a significant effect on the gaseous products. Generally, the effect of pressure on coal pyrolysis is not significant, compared to its effect on the chemical reactions. Thus a good approximation is to apply the pyrolysis kinetics at low-pressure conditions for high pressure; however, different coals have different pyrolysis behaviors. To select the appropriate kinetic for the coal under study, the experimental kinetic parameters for different coals were examined, and the effects of pyrolysis kinetics on the UCG process in large coal blocks were investigated. The results of this part are discussed in more detail in Section 5.

## 4. Parameter estimation

As discussed in Section 2.3, eleven reactions (two pyrolysis and nine chemical reactions) were considered in the model. All these reactions occur in UCG simultaneously and are modeled with an Arrhenius type reaction. The chemical processes are sensitive to the coal block size and the environment condition where the reaction occurs. Any change in the coal block size has a significant effect on the modeling results.

To best represent and model UCG for the field scale, the chemical kinetics, which were obtained in the laboratory, are required to be estimated or upscaled for field scale. From an engineering point of view, this is an inverse problem, where the aim is the determination of the model parameter(s) within a certain domain from data and information provided as final results. In UCG, we deal with an inverse problem: The model response, which is the produced gas composition, is already known from field data, and it is necessary to estimate reaction parameters based on these results. As noted earlier, the Levenberg–Marquardt algorithm (LMA) is selected for parameter estimation. This algorithm is a technique that finds the minimum of a function, generally nonlinear, over a set of function parameters. This technique is usually applicable for least squares curve fitting and nonlinear programming. Like other numeric minimization algorithms, the LMA is an iterative procedure.

As an optimization method, the LMA can be considered as a combination of the steepest descent and Gauss–Newton methods. When the initial guess is far from the solution, the algorithm behaves like the steepest descent method: It has a linear convergence rate, but it is guaranteed to converge. When the initial guess is close to the correct solution, it behaves like the Gauss–Newton method with a quadratic convergence.

Overall, the LMA is more powerful than the Gauss–Newton method. In many cases, it can find a solution, even if the initial guess is very far off the final minimum (Lourakis, 2005).

To start a minimization, an initial guess for the parameters must be provided. For instance, reaction kinetics at low pressure with fine particles can be used as an initial guess to estimate parameters for high pressure and large coal blocks. The produced gas mole fractions, using a forward model, are selected as the model response; these results must be matched with the field gas composition. The produced gas composition should be extracted at different times, because the produced gases are not uniform over time. One may consider the whole process interval, using 5 or 10 specific times to monitor the produced gases at those times.

The frequency factor is the parameter to be estimated at high-pressure conditions. As noted earlier, the activation energy remains almost constant when increasing the pressure. The aim is the estimation and upscaling of the frequency factors by the LMA method. Table 3 summarizes the reaction kinetics that are used as the initial guess in the LMA. The theory and equations for the LMA are described in the following paragraphs.

The experimental and modeling results are defined as

$$\omega^{\text{exp}} = [\omega_{\text{CO}_2, t_1}^{\text{exp}} \quad \omega_{\text{CH}_4, t_1}^{\text{exp}} \quad \omega_{\text{CO}, t_1}^{\text{exp}} \quad \omega_{\text{H}_2, t_1}^{\text{exp}} \quad \omega_{\text{CO}_2, t_2}^{\text{exp}} \quad \omega_{\text{CH}_4, t_2}^{\text{exp}} \quad \omega_{\text{CO}, t_2}^{\text{exp}} \quad \omega_{\text{H}_2, t_2}^{\text{exp}} \quad \dots]^T$$

and

$$\omega = [\omega_{\text{CO}_2, t_1} \quad \omega_{\text{CH}_4, t_1} \quad \omega_{\text{CO}, t_1} \quad \omega_{\text{H}_2, t_1} \quad \omega_{\text{CO}_2, t_2} \quad \omega_{\text{CH}_4, t_2} \quad \omega_{\text{CO}, t_2} \quad \omega_{\text{H}_2, t_2} \quad \dots]^T$$

where  $\omega_{i, t_j}$  is the mole fraction of the produced gas  $i$  at specific time  $t_j$ .

As discussed before, the primary application of the LMA is for least squares curve fitting. Thus, as parameters and responses are defined, the next step is the definition of an objective function that is to be minimized. Defining a set of empirical data pairs of independent and dependent variables to optimize the parameters of the model, the sum of the squares of the deviation becomes minimal. For UCG, the aim is minimization of the difference between the gas composition of the field data and the results obtained from the numerical forward model. Based on this consideration, the objective function is defined as

$$M = (\omega^{\text{exp}} - \omega)^T (\omega^{\text{exp}} - \omega) = \sum_{m=1}^M \sum_{i=1}^I (\omega_{m,i}^{\text{exp}} - \omega_{m,i})^2 \quad (22)$$

To minimize the objective function, its derivative with respect to the dependent variables must be zero:

$$\frac{\partial S(\varepsilon)}{\partial \varepsilon_1} = \frac{\partial S(\varepsilon)}{\partial \varepsilon_2} = \dots = 0 \quad (23)$$

The sensitivity matrix is defined as

$$J(\varepsilon) = \begin{bmatrix} \frac{\partial \omega_{t_1}}{\partial \varepsilon_1} & \frac{\partial \omega_{t_1}}{\partial \varepsilon_2} & \dots & \frac{\partial \omega_{t_1}}{\partial \varepsilon_{i-1}} & \frac{\partial \omega_{t_1}}{\partial \varepsilon_i} \\ \frac{\partial \omega_{t_2}}{\partial \varepsilon_1} & \frac{\partial \omega_{t_2}}{\partial \varepsilon_2} & \dots & \vdots & \vdots \\ \frac{\partial \omega_{t_3}}{\partial \varepsilon_1} & \frac{\partial \omega_{t_3}}{\partial \varepsilon_2} & \dots & \vdots & \vdots \\ \vdots & \vdots & \dots & \vdots & \vdots \\ \frac{\partial \omega_{t_j}}{\partial \varepsilon_1} & \frac{\partial \omega_{t_j}}{\partial \varepsilon_2} & \dots & \frac{\partial \omega_{t_j}}{\partial \varepsilon_{i-1}} & \frac{\partial \omega_{t_j}}{\partial \varepsilon_i} \end{bmatrix} \quad (24)$$

where

$$\omega_{t_j} = [\omega_{\text{CO}_2, t_j} \quad \omega_{\text{CH}_4, t_j} \quad \omega_{\text{CO}, t_j} \quad \omega_{\text{H}_2, t_j}]^T \quad (25)$$

Finally, the linear system of algebraic equations to obtain the next set of kinetic parameters is

$$[(J^v)^T J^v + \sigma^v \Omega^v] \Delta \varepsilon^v = (J^v)^T [\omega^{\text{exp}} - \omega(\varepsilon^v)] \quad (26)$$

where

$$\Omega^v = \text{diag}[(J^v)^T J^v] \quad (27)$$

In Eq. (26),  $\Delta \varepsilon^v$  is the difference between the new kinetic parameters and the old input parameters; therefore, the new kinetic parameters can be calculated from the input data. Fig. 4 illustrates the LMA as a flowchart, which details the parameter estimation for the gasification process. Combination of forward model with LMA allows a fast optimization of the UCG process and the determination of the optimal reaction parameters; the model predictions for the produced gas composition are compared with the field data.

Based on the above discussion, the frequency factors are considered as the uncertain parameters for estimation. An initial guess for the frequency factors is introduced into the forward model, and the result (gas composition) from the forward model is then interposed to the LMA to generate a new set of frequency factors. To construct a sensitivity analysis (matrix  $J$ ), it is essential to investigate the effect of each individual reaction on the process. To analyze the sensitivity of each frequency factor, in each step, the frequency factor for one reaction is changed, and the frequency factors for other reactions are kept constant. This procedure is repeated for all reaction frequency factors, and the corresponding produced gas compositions by the forward model are obtained. Now, the entries in the sensitivity matrix are calculated by a simple numerical derivative, and the sensitivity matrix is formed.

Eq. (26) is applied to the initial guess for the parameters – the field produced gas composition and the results from the forward model – to estimate a new set of parameters. If the new estimates improve the forward model results, these parameters are accepted, and the iteration is continued. Otherwise, the adjusting parameter ( $\sigma$ ) is increased or decreased to improve the model results. The aim is the estimation of a set of frequency factors that result in the field produced gas composition; therefore, the above procedure is repeated until a good agreement between the forward model and field results is achieved.

## 5. Results and discussion

### 5.1. Pyrolysis process sensitivity study

To analyze the sensitivity of the model with respect to different pyrolysis kinetics, chemical reactions and their parameters remain the same, while the pyrolysis kinetic parameters are varied. Table 4 summarizes the kinetics parameters that are obtained from laboratory experimental studies for different coals, based on treating a simple first-order Arrhenius reaction for pyrolysis.

Eight different sets of pyrolysis kinetics, including frequency factor and activation energy, are considered. The effect of different pyrolysis kinetics on the produced gas mole fraction is analyzed and illustrated as a bar chart (Fig. 5). It should

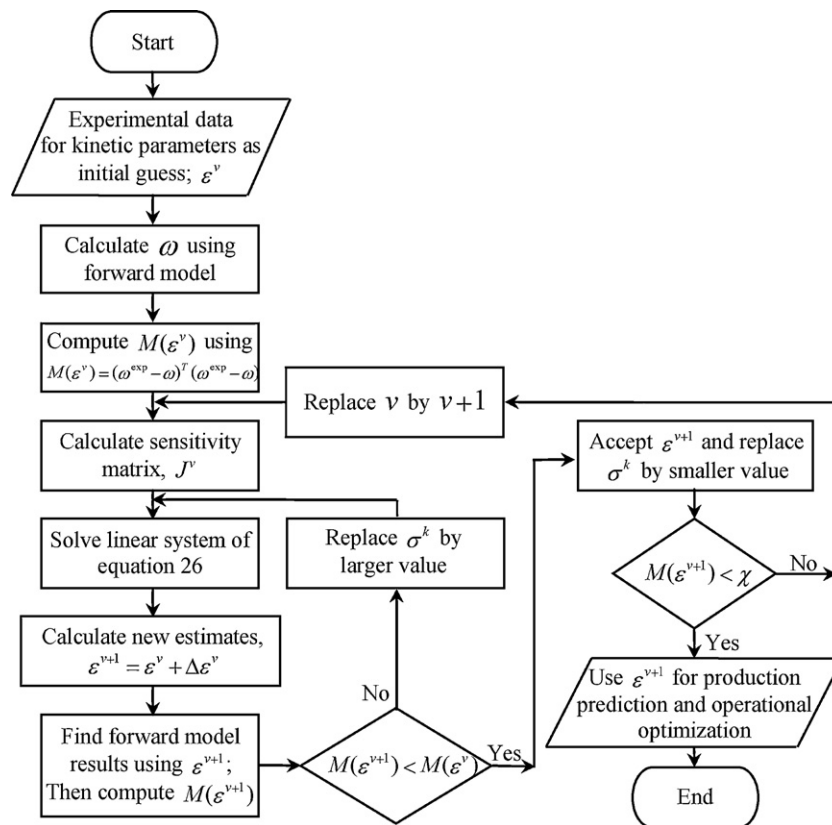


Fig. 4 – LMA method for parameter estimation in UCG.

be noted that pyrolysis is modeled as a single reaction and that all pyrolysis gases are produced by a single reaction. Fig. 5 illustrates the composition of carbon monoxide, which is almost independent of the pyrolysis reaction: For all kinetics, its value is about 0.09 mole fraction. The reason is that carbon monoxide, which is produced in the pyrolysis process, is much less than its production during the gasification process. Thus any change in carbon monoxide produced by pyrolysis has a minor effect on the total amount of carbon monoxide that is produced during the gasification process.

Variation of the methane mole fraction is not really considerable, either. This is due to the production of methane in the hydrogenation reaction, rather than in pyrolysis alone, at high-pressure gasification. This behavior is not the same at low pressures, while the produced methane during the UCG process is mainly due to the pyrolysis of coal methane.

The gas composition for carbon dioxide, methane and hydrogen in pyrolysis 4 reveals that the pyrolysis starting temperature affects the char gasification process. As the process continues, most of the hydrogen reacts with char to produce methane, the available char for carbon combustion decreases,

and carbon dioxide is reduced. The hydrogen mole fraction shows relatively higher variation with respect to pyrolysis kinetics, compared to other produced gases, but its variation is less than 5 percent.

Overall, different pyrolysis kinetics have a minor effect on the mole fractions of the produced gases, which is due to the nature of the gasification process where the amount of gas produced in the pyrolysis process is not comparable to the total amount of gases in the gasification process. It should be mentioned that the pyrolysis process controls the rate of char reaction. The availability of carbon for char reactions is dominated by pyrolysis. As carbon is produced by pyrolysis, this process no longer has a significant effect on the gasification process.

Based on the above discussion, for a large coal block, the main criterion for selection of the pyrolysis process kinetics is the selection of parameters in which the process occurs within an appropriate temperature range with a controlled gasification rate. If pyrolysis starts at a low temperature, gasification occurs on a large portion of the coal seam, which is not according to the nature of the process. Otherwise, gasification will

Table 4 – Kinetic parameters for modeling of pyrolysis by simple reaction.

Reference	K	E	Starting temp.	Ending temp.	No
Van Krevelen et al. (1951)	$10^7$	135.90	400	520	1
Boyer (1952)	$10^{11}$	188.28	400	500	2
Stone et al. (1954)	$5.41 \times 10^6$	114.22	430	500	3
Shapatina et al. (1960)	11	15.060	380	560	4
Howard and Essenhig (1967)	5.37	14.210	600	1000	5
Wiser et al. (1967)	47.5	62.760	440	500	6
Badzioch and Hawksley (1970)	$1.14 \times 10^5$	74.480	650	820	7
Anthony et al. (1976)	$1.8 \times 10^3$	55.650	450	1000	8



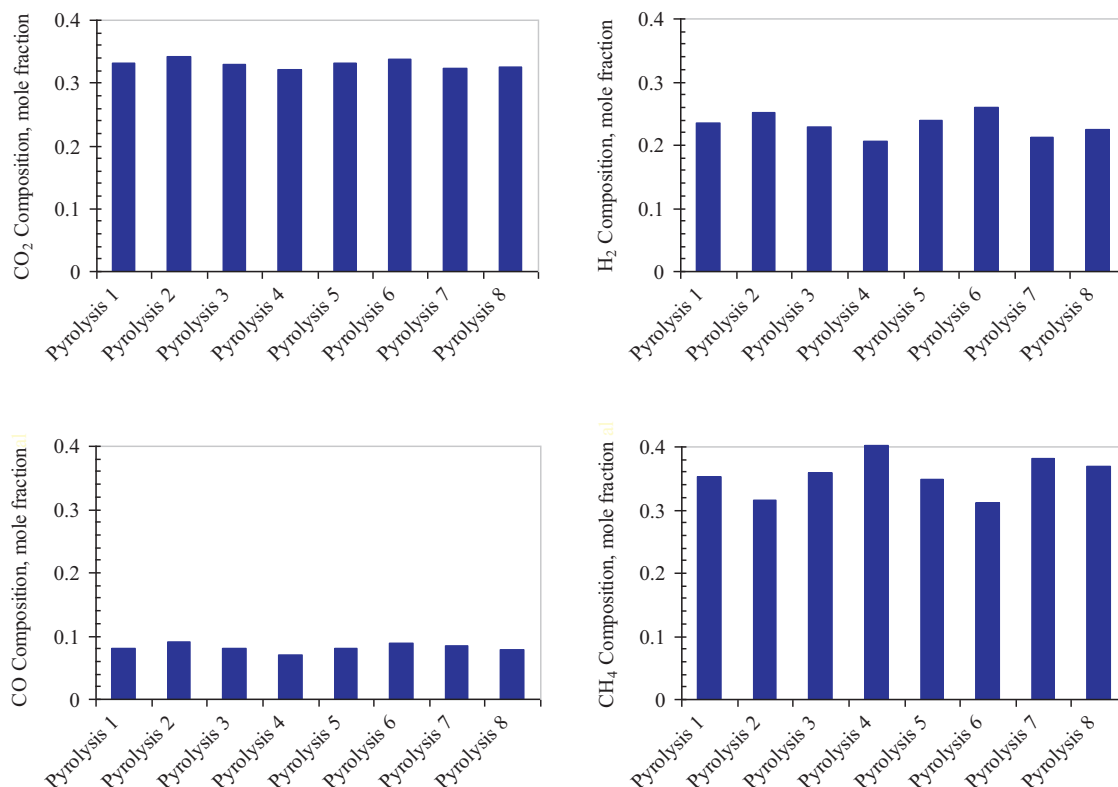


Fig. 5 – Produced gas composition for different pyrolysis kinetics.

not start if pyrolysis occurs at a high temperature. These properties are satisfied by reported kinetics number 2. During this study, these parameters are assigned to the pyrolysis process.

## 5.2. Reaction rate sensitivity study

A comprehensive sensitivity study prior to parameter estimation is crucial. This sensitivity study enables us to investigate the effect of different parameters on the model behavior and provides us with an idea(s) for parameter estimation. Nine reactions are considered for chemical processes: The reaction kinetics for pyrolysis is fixed and not considered for parameter estimation. The reaction kinetics (frequency factor) for chemical reactions are the main parameters under study. As a sensitivity study, the effect of each reaction rate on the produced gas composition is investigated. In each step, the kinetic parameters of all reactions except the one under study are kept constant, and the rate of the desired reaction on the produced gas is analyzed.

The results of the sensitivity study for nine chemical reactions are shown in Fig. 6, which illustrates the sensitivity of the produced gases with respect to each individual reaction. The x-axis shows the dimensionless time, which is calculated by dividing the process time by the total time, and the y-axis shows the change in gas composition as the rate of reaction varies. The sensitivity study is carried out for different gases, which are identified by different colors.

The values on the y-axis describe the sensitivity of different gases with respect to a specific reaction. A higher deviation from zero reveals a significant effect of that reaction on the produced gas composition. For instance, the rate of the Boudouard reaction ( $R_2$ ) significantly affects the carbon monoxide, carbon dioxide, and methane mole fractions, while it has no effect on the hydrogen mole fraction. Increasing the rate of the Boudouard reaction enhances the carbon monoxide

mole fraction and reduces the carbon dioxide and methane mole fractions. For the Boudouard reaction, the effect of the reaction rate is almost stable with respect to time, and the value on the y-axis shows almost a constant number.

For some other reactions, however, the effect of the reaction rate is strongly time dependent. For instance, the mole fractions of the produced gases are a weak function of the steam gasification rate ( $R_4$ ) in the first half of the process ( $0.6T_D$ ), becoming significant later in the process.

In summary, this sensitivity study enables us to predict the process behavior by changing reaction kinetics. The mole fractions of the produced gases can be estimated by changing the reaction rates. If a new reaction rate and a sensitivity graph are available, it is possible to predict the mole fraction of the produced gas with respect to the change in the reaction rate.

## 5.3. Estimated kinetics

The frequency factors are estimated based on the field gas compositions as experimental results. Parameter estimation is an iterative process, and the accuracy of the predicted results compared to the field data dictates the number of iterations. It is not possible to illustrate the results at each iteration; thus, the initial guess and final results are considered in this manuscript. The initial kinetic parameters obtained from the literature data at low pressure are summarized in Table 3, and the final kinetics for all chemical reactions is given in Table 5. To best estimate these parameters (with greater accuracy), the LMA requires more iterations, which leads to a higher computational time.

Table 6 illustrates the average gas composition for the field and the forward model. The model results for the initial and final estimated kinetics are also shown in Fig. 7 for comparison. As the results indicate, the kinetic parameters for low pressures (initial guess) predict carbon dioxide appropriately,

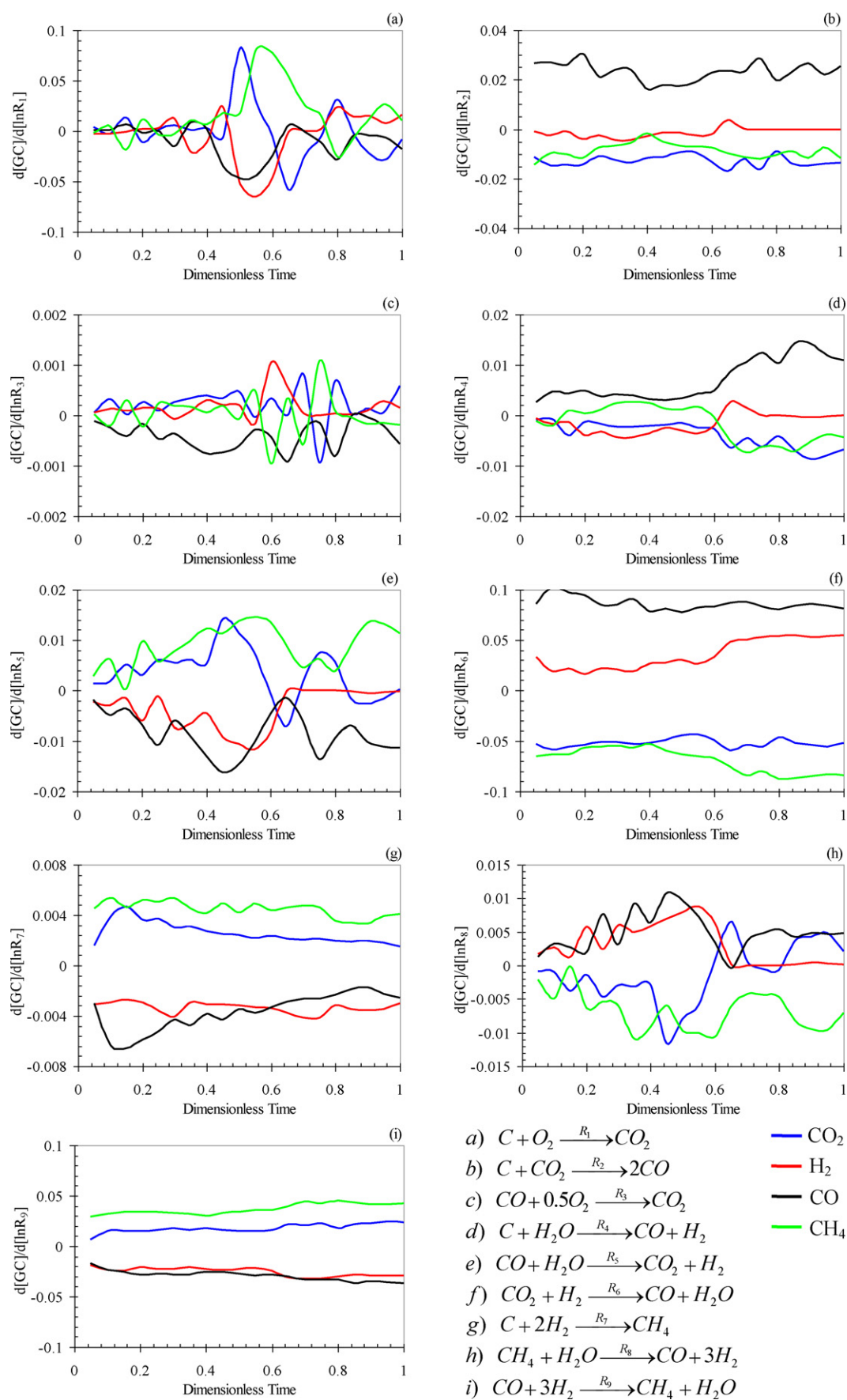
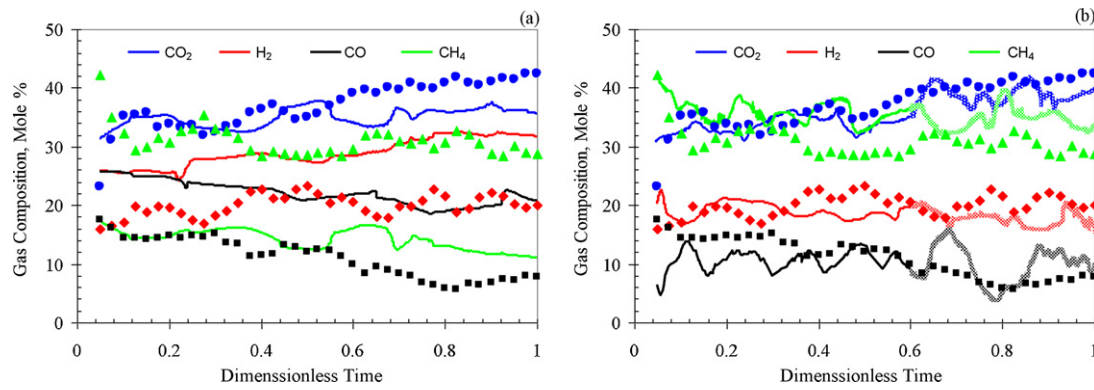


Fig. 6 – Sensitivity of produced gases for different reactions.



**Fig. 7 – Simulated (—) vs. typical field (●) gas composition; (a) initial guess for kinetic parameters and (b) estimated kinetic parameters.**

**Table 5 – Estimated chemical kinetic parameters.**

Reaction	Activation energy	Reaction frequency factor
$C + O_2 \rightarrow CO_2$	100	$2.08 \times 10^1$
$C + CO_2 \rightarrow 2CO$	249	$6.57 \times 10^6$
$C + H_2O \rightarrow CO + H_2$	156	$1.87 \times 10^4$
$C + 2H_2 \rightarrow CH_4$	200	$1.81 \times 10^3$
$CO + 0.5O_2 \rightarrow CO_2$	247	$1.12 \times 10^8$
$CO + H_2O \rightarrow CO_2 + H_2$	12.6	$1.73 \times 10^0$
$CO_2 + H_2 \rightarrow CO + H_2O$	12.6	$4.48 \times 10^{-2}$
$CH_4 + H_2O \rightarrow CO + 3H_2$	30.0	$3.13 \times 10^2$
$CO + 3H_2 \rightarrow CH_4 + H_2O$	30.0	$4.00 \times 10^3$

but over-predict hydrogen and carbon monoxide and under-predict methane gas composition. The estimated kinetics improves the produced gas composition and reduces the difference between the modeling result and the field data. The best agreement is obtained for carbon dioxide and is followed by hydrogen, carbon monoxide, and methane, respectively. The coal seam is saturated with water and methane; therefore, an error in the initial methane saturation can cause error in the produced gas composition. A part of the error in the methane prediction can be attributed to an error in the initial methane calculation. To fit the modeling result more appropriately, more iterations are required.

Reactions in UCG are not independent, thus there is possibility to have more than one solution for this process. To obtain a set of reaction kinetics, two steps are considered. First, reaction kinetics at low pressure condition is selected as initial guess. Second step is to use a part of production data for estimating reaction kinetics and the rest of production data for parameters validation. For instance, if there are 12 months of production data, the parameters are estimated by first 8 months of production data and next 4 months used to compare the predicted results with field data. If estimated reaction kinetics can predict the second part of production data, which is not used for parameter estimation, then it is expected that estimated reaction kinetics will predict future performance of process more realistically. Fig. 7 illustrates the gas composition for initial and final estimated parameters over the entire

process. The dots show a typical field gas composition while the lines are predicted (simulated) results. Fig. 7(a) shows simulation results correspond to the initial guess. As depicted in the figure there is a large difference between predicted result and field data. This set of parameters is introduced to parameter estimation algorithm and after some iteration the final result is obtained (Fig. 7(b)). In this case, the kinetic parameters are estimated based on 60% of production data (up to  $T_D = 0.6$ ), which is shown by solid line, and the rest of data are predicted with new kinetics (shaded line). Comparing the Fig. 7(a) and (b) demonstrate that there is a good agreement between the gas compositions; only the methane composition is over predicted. As mentioned earlier, the coal is saturated with water and methane, therefore, an error in the initial methane saturation can cause error in the produced gas composition.

At the end, it should be mentioned that the kinetic parameters, which are estimated here, are not unique and this set of parameters is obtained based on production data. More production data can provide more reliable set of kinetic parameters, therefore new production data can be used to update and modify kinetic parameters.

#### 5.4. Cavity shape and temperature profile

As a preliminary study, this work focuses on the simulation of a pilot test area. The cavity shape and temperature profile were examined in the study by Nourozieh et al. (2010). The results illustrated the feasibility of the UCG process for the coal seam under consideration. Fig. 8 shows the cavity shape and porosity distribution after ten days simulation based on the obtained kinetic parameters. The ignition happens at the toe of the horizontal injector where there is a high permeability region between the wells. As the process proceeds, the injection point is perforated at successive new upstream locations. As this figure shows, a single cavity is formed along the coal seam. The cavity grows along the x-axis much more than along the z-axis, which depends on the geological structure and ignition procedure. The shale layer affects the rate of the cavity growth in the vertical direction; however, there is a vertical penetration for the gasification in the middle coal seam. In addition, the backward gasification along the x-axis is faster than the forward gasification.

There is an area (red region) in Fig. 8 where all the coal has been gasified. The cavity temperature profile is illustrated in Fig. 9. The temperature inside the cavity indicates different regions during UCG. These regions are separated by lines in Fig. 9. The pyrolysis region has a temperature around 500 °C during this study. This agrees with the study of Anthony and

**Table 6 – Average gas composition before and after parameter estimation.**

	CO <sub>2</sub>	H <sub>2</sub>	CO	CH <sub>4</sub>
Field results	0.3700	0.2000	0.1200	0.3100
Initial guess for kinetics	0.3491	0.2887	0.2206	0.1416
Estimated parameters	0.3577	0.1850	0.0961	0.3612

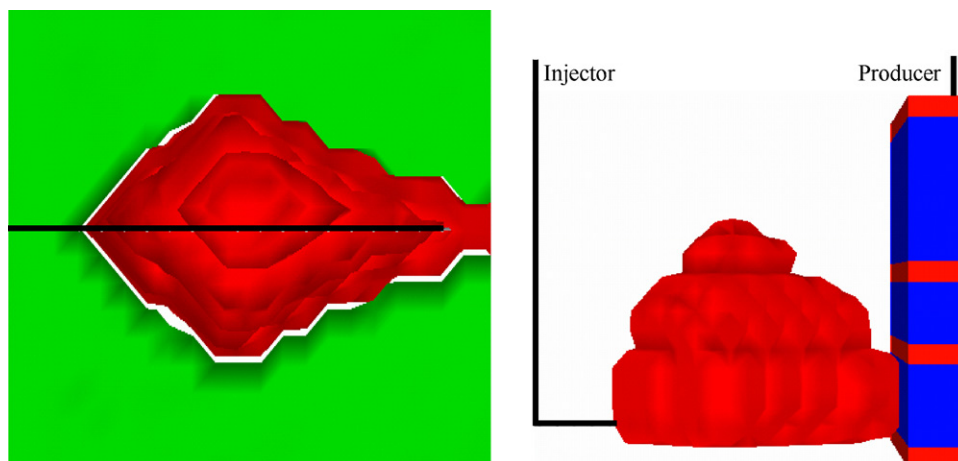


Fig. 8 – Cavity shape after 10 days simulation; x-z cross (right) and x-y cross (left) (Nourozieh et al., 2010).

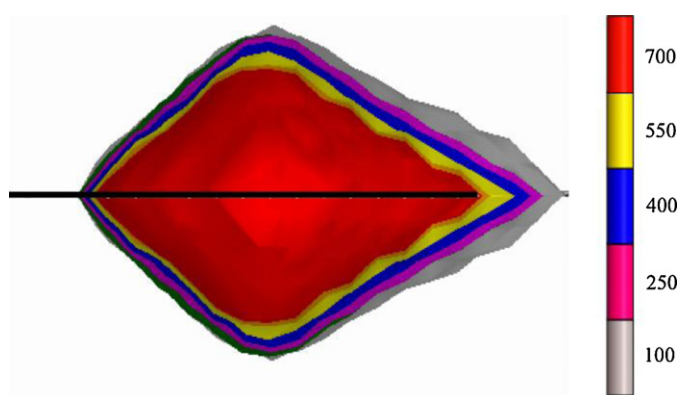


Fig. 9 – Cavity temperature profile (°C) after 10 days simulation (Nourozieh et al., 2010).

Howard (1976) which reported a temperature of 400–900 °C for pyrolysis during UCG.

After the pyrolysis is complete, the porous carbonaceous rich solid referred to as char is reacted with gases inside the cavity. The temperature in Fig. 9 confirms that the char gasification occurs at a temperature of around 700 °C. Thus, this process happens right after the pyrolysis is complete at temperature 500 °C.

## 6. Conclusions

A new method for kinetic reaction estimation at high pressure underground coal gasification has been proposed. This method combines a numerical forward model and field data to estimate uncertain chemical kinetic parameters. The novelty of the developed method is in its applicability as well as its ability to generate the chemical reaction kinetics based on field or pilot data. A comprehensive sensitivity study for the reaction kinetics and pyrolysis process has been carried out, and the model's response to those parameters has been investigated. The pyrolysis process at low pressure can be used for high-pressure conditions provided that the temperature range is selected appropriately. Reaction kinetics must be modified for high pressures and the environment condition in which the reactions occur. The model's produced gas composition based on the estimated parameters has been compared with the field data, and there is a good agreement between modeling and field data which shows that the proposed method

converges to solution. The developed model can be used for studying the UCG process in the field scale and for design and optimization of this process.

## Acknowledgements

The authors would like to thank Dr. Hassan Hassanzadeh for helpful discussions during preparation of the manuscript. The authors also acknowledge the technical support of Computer Modelling Group (CMG) Ltd., Calgary, Canada. The support of the Natural Sciences and Engineering Research Council of Canada (NSERC), the Schulich School of Engineering, and NSERC/AERI/iCORE/Foundation CMG Chair Funds are acknowledged.

## References

- Anthony, D.B., Howard, J.B., 1976. Coal devolatilization and hydrogasification. *AIChE J.* 22 (4), 625–656.
- Anthony, D.B., Howard, J.B., Hottel, H.C., Meissner, H.P., 1976. Rapid devolatilization and hydrogasification of bituminous coal. *Fuel* 55 (2), 121–128.
- Badzioch, S., Hawksley, P.G.W., 1970. Kinetics of thermal decomposition of pulverized coal particles. *Ind. Eng. Chem. Process Des. Dev.* 9 (4), 521–530.
- Blasi, C.D., 2000. Dynamic behavior of stratified downdraft gasifiers. *Chem. Eng. Sci.* 55 (15), 2931–2944.
- Boyer, M.S.F., 1952. *Compt. Rend. Assoc. Tech. de l'Indus. du gaz en France Congres.*, p. 653 (as reported by Anthony and Howard (1976)).
- Burton, E., Friedmann, J., Upadhye, R., 2006. *Best Practices in Underground Coal Gasification*. Lawrence Livermore National Laboratory, Livermore, CA (Contract No.: W-7405-Eng-48).
- Campbell, J.H., 1978. Pyrolysis of subbituminous coal in relation to in-situ coal gasification. *Fuel* 57 (4), 217–224.
- Energy Resources Conservation Board, June 2008. ST98-2008: Alberta's energy reserves 2007 and supply/demand outlook 2008–2017. <http://www.ercb.ca/docs/products/sts/st98-2008.pdf>
- Govind, R., Shah, J., 1984. Modeling and simulation of an entrained flow coal gasifier. *AIChE J.* 30 (1), 79–92.
- Gregg, D.W., Edgar, T.F., 1978. Underground coal gasification. *AIChE J.* 24 (5), 753–781.
- Hawley, M.C., Boyd, M., Anderson, C., DeVera, A., 1983. Gasification of wood char and effects of intraparticle transport. *Fuel* 62 (2), 213–216.
- Howard, J.B., Essenhight, R.H., 1967. Pyrolysis of coal particles in pulverized fuel flames. *Ind. Eng. Chem. Process Des. Dev.* 6 (1), 74–84.



- Kumar, M., Gupta, R.C., 1994. Influence of carbonization conditions on the gasification of acacia and eucalyptus wood chars by carbon dioxide. *Fuel* 73 (12), 1922–1925.
- Levenberg, K., 1944. A method for the solution of certain non-linear problems in least squares. *Quart. Appl. Math.* 2, 164–168.
- Lourakis, M., 2005. A brief description of the Levenberg–Marquardt algorithm implemented by Levmar. <http://www.ics.forth.gr/~lourakis/levmar/levmar.pdf>
- Lyczkowski, R.W., 1978. Mechanistic Theory for Drying of Porous Media. Lawrence Livermore National Laboratory, Livermore, CA (Report No.: UCRL-52456).
- MacNeil, S., Basu, P., 1998. Effect of pressure on char combustion in a pressurized circulating fluidized bed boiler. *Fuel* 77 (4), 269–275.
- Makino, M., Toda, Y., 1979. Factors affecting methane evolution on pyrolysis of coal under pressure. *Fuel* 58 (3), 231–234.
- Marquardt, D., 1963. An algorithm for least-squares estimation of nonlinear parameters. *SIAM J. Appl. Math.* 11 (2), 431–441.
- Marquez-Montesinos, F., Cordero, T., Rodriguez-Mirasol, J., Rodriguez, J.J., 2002. CO<sub>2</sub> and steam gasification of a grapefruit skin char. *Fuel* 81 (4), 423–429.
- Massaquoi, J.G.M., Riggs, J.B., 1983a. Mathematical modeling of combustion and gasification of a wet coal slab—I: model development and verification. *Chem. Eng. Sci.* 38 (10), 1747–1756.
- Massaquoi, J.G.M., Riggs, J.B., 1983b. Mathematical modeling of combustion and gasification of a wet coal slab—II: mode of combustion, steady state multiplicities and extinction. *Chem. Eng. Sci.* 38 (10), 1757–1766.
- Moilanen, A., Saviharju, K., 1997. Gasification reactivities of biomass fuels in pressurized conditions and product gas mixtures. In: Bridgwater, A.V., Boocock, D.G.B. (Eds.), *Developments in Thermochemical Biomass Conversion*. Blackie A & P, London, pp. 828–837.
- Monson, C.R., Germane, G.J., Blackham, A.U., Smoot, L.D., 1995. Char oxidation at elevated pressures. *Combust. Flame* 100 (4), 669–683.
- Muhlen, H.J., van Heek, K.H., Juntgen, H., 1985. Kinetic studies of steam gasification of char in the presence of H<sub>2</sub>, CO<sub>2</sub> and CO. *Fuel* 64 (7), 944–949.
- Nourozieh, H., Kariznovi, M., Chen, Z., Abedi, J., 2010. Simulation study of underground coal gasification in Alberta Reservoirs: geological structure and process modeling. *Energ. Fuel* 24 (6), 3540–3550.
- Park, K.Y., Edgar, T.F., 1987. Modeling of early cavity growth for underground coal gasification. *Ind. Eng. Chem. Res.* 26 (2), 237–246.
- Perkins, G., Sahajwalla, V., 2005. A mathematical model for the chemical reaction of a semi-infinite block of coal in underground coal gasification. *Energ. Fuel* 19 (4), 1679–1692.
- Roberts, D.G., Harris, D.J., 2000. Char gasification with O<sub>2</sub>, CO<sub>2</sub>, and H<sub>2</sub>O: effects of pressure on intrinsic reaction kinetics. *Energ. Fuel* 14 (2), 483–489.
- Rodriguez-Mirasol, J., Cordero, T., Rodriguez, J.J., 1993. CO<sub>2</sub>-reactivity of eucalyptus Kraft lignin chars. *Carbon* 31 (1), 53–61.
- Schulze-Riege, R.W., Haase, O., Nekrasov, A., 2003. Combined global and local optimization techniques applied to history matching. In: *Proceeding of the SPE Reservoir Simulation Symposium*, February 3–5, Houston, TX (SPE 79668-MS).
- Shafirovich, E., Varma, A., 2009. Underground coal gasification: a brief review of current status. *Ind. Eng. Chem. Res.* 48 (17), 7865–7875.
- Shapatina, E.A., Kalyuzhnyi, V.A., Chukhanov, Z.F., 1960. Technological utilization of fuel for energy I—thermal treatment of fuels (as reported by Anthony and Howard (1976)).
- Shufen, L., Ruizheng, S., 1994. Kinetic studies of a lignite char pressurized gasification with CO<sub>2</sub>, H<sub>2</sub> and steam. *Fuel* 73 (3), 413–416.
- Smith, I.W., 1978. The intrinsic reactivity of carbons to oxygen. *Fuel* 57 (7), 409–414.
- Stone, H.N., Batchelor, J.D., Johnstone, H.F., 1954. Low temperature carbonization rates in a fluidized bed. *Ind. Eng. Chem.* 46 (2), 274–278.
- Tancredi, N., Cordero, T., Rodriguez-Mirasol, J., Rodriguez, J.J., 1996. CO<sub>2</sub> gasification of eucalyptus wood chars. *Fuel* 75 (13), 1505–1508.
- Tomita, A., Mahajan, O.P., Walker Jr., P.L., 1977. Reactivity of heat-treated coals in hydrogen. *Fuel* 56 (2), 137–144.
- Tsang, T.H.T., 1980. Modeling of heat and mass transfer during coal block gasification. PhD thesis. The University of Texas at Austin, Austin, TX.
- Van Krevelen, D.W., Van Heerden, C., Huntjens, F.J., 1951. Physicochemical aspects of the pyrolysis of coal and related organic compounds. *Fuel* 30 (11), 253–259.
- Wiser, W.H., Hill, G.R., Kertamus, N.J., 1967. Kinetic study of pyrolysis of high volatile bituminous coal. *Ind. Eng. Chem. Process Des. Dev.* 6 (1), 133–138.
- Yang, L., Liu, S., 2003. Numerical simulation on heat and mass transfer in the process of underground coal gasification. *Numer. Heat Transfer A: Appl.* 44 (5), 537–557.
- Zolin, A., Jensen, A., Jensen, P.A., Frandsen, F., Johansen, K.D., 2001. The influence of inorganic materials on the thermal deactivation of fuel chars. *Energ. Fuel* 15 (5), 1110–1122.